Analytical solutions for Newtonian and inelastic non-Newtonian flows with wall slip

L.L. Ferrás [a], J.M. Nóbrega [a,*], F.T. Pinho [b]

[a] IPC – Institute for Polymers and Composites, University of Minho, Campus de Azurém, 4800-058 Guimarães, Portugal
[b] Centro de Estudos de Fenómenos de Transporte, Faculdade de Engenharia da Universidade do Porto, Rua Dr. Roberto Frias s/n, 4200-465 Porto, Portugal

ABSTRACT

This work presents analytical solutions for both Newtonian and inelastic non-Newtonian fluids with slip boundary conditions in Couette and Poiseuille flows using the Navier linear and non-linear slip laws and the empirical asymptotic and Hatzikiriakos slip laws. The non-Newtonian constitutive equation used is the generalized Newtonian fluid model with the viscosity described by the power law, Bingham, Herschel–Bulkley, Sisko and Robertson–Stiff models. While for the linear slip model it was always possible to obtain closed form analytical solutions, for the remaining non-linear models it is always necessary to obtain the numerical solution of a transcendent equation. Solutions are included with different slip laws or different slip coefficients at different walls.

© 2012 Elsevier B.V. All rights reserved.

1. Introduction

Wall slip occurs in many industrial applications, such as in polymer extrusion processes, thus affecting the throughput and the quality of the final product [1]. Therefore, analytical solutions of slip in shear flows are important to solve relevant industrial problems and better understand them, but also for the assessment of computational codes used in fluid flow simulations. There are many exact solutions for fluid flow in the literature [2,3] some of which are very simple, and others that use complex rheological models [3]. Even though the simple exact solutions seem trivial, they are the building blocks to the understanding of more complex solutions. They usually rely on the Dirichlet type (no-slip) boundary condition (**u** = **0**, where **u** stands for the velocity at the wall). However, there is experimental evidence suggesting that some fluids do not obey this condition at the wall [4], and show instead slip along the wall. For a review on wall slip with non-Newtonian fluids, including slip laws and techniques to measure this property, the works of Denn [1], Lauga et al. [4] and Hatzikiriakos [5] are strongly advised.

Meijer and Verbraak [6] and Potente et al. [7,8] present analytical solutions for Poiseuille flow in extrusion using wall slip for Newtonian and power law fluids. Chatzimina et al. [9] solves for non-linear slip in annular flows and analyses its stability. Ellahi et al. [10] presents an analytical solution for viscoelastic fluids described by the 8-constant Oldroyd constitutive equation with non-linear wall slip. Wu et al. [11] investigated analytically the pressure driven transient flow of Newtonian fluids in microtubes with Navier slip, whereas Mathews and Hill [12] presented analytical solutions for pipe, annular and channel flows with the slip boundary conditions given by Thompson and Troian [13]. Yang and Zhu [14], and the references cited therein, report analytical solutions and theoretical studies of squeeze flow with the Navier slip boundary condition. It is also worth mentioning the works on the well-posedness of the Stokes equations with leak, slip and threshold boundary conditions [15,16], which also included their numerical implementation.

In spite of the wealth of solutions in the literature, there is a wide range of slip conditions, which have not been addressed analytically. With the exception of the simple linear Navier slip, for most other slip laws in the literature the analytical solutions for the so-called indirect problem are missing. Here, the results are dependent on the imposed flow rate. For the direct problem the literature is rich on the solutions [6–11] but lack the corresponding reverse case, and this is not just a matter of inverting the final expressions because of the non-linearity of the slip models and of the constitutive equations. In fact, the inverse problem is invariably more difficult to obtain than the solution of the direct problem. The main purpose of this paper is precisely to address these issues and report some new analytical solutions in particular for the inverse problem.

The remainder of this paper is organized as follows: Section 2 presents the governing equations and the employed slip models. The study of Newtonian fluid flows with slip is presented first in Section 3, starting with the simple Couette flow for the sake of understanding and this is followed by the Poiseuille flow using linear and non-linear slip boundary conditions and different slip coefficients at the upper and bottom walls (the existing relevant

* Corresponding author. Tel.: +351 253510320; fax: +351 253510339.
E-mail addresses: luis.ferras@dep.uminho.pt (L.L. Ferrás), mnobrega@dep.uminho.pt (J.M. Nóbrega), fpinho@fe.up.pt (F.T. Pinho).

literature [6–8] is only concerned with the direct problem for melt flow in extrusion screws). Section 3 ends with a study of Newtonian Poiseuille flow with the Hatzikiriakos and asymptotic slip laws and is followed by Section 4 which describes solutions for the generalized Newtonian model with the viscosity function given by power law [17], Sisko [18], Herschel and Bulkley (Bingham) [19] and Robertson and Stiff [20] models, both for linear and non-linear slip models. The text ends with the conclusions, in Section 5.

2. Theory

2.1. Governing equations

This work concerns incompressible fluids which are governed by the continuity equation

$$\nabla \cdot \mathbf{u} = 0, \tag{1}$$

and the momentum equation

$$\frac{\partial(\rho\mathbf{u})}{\partial t} + \rho\nabla \cdot \mathbf{u}\mathbf{u} = -\nabla p + \nabla \cdot \boldsymbol{\tau}. \tag{2}$$

In Eq. (2) $\mathbf{u}$ is the velocity vector, p is the pressure, $\boldsymbol{\tau}$ is the deviatoric stress tensor and the gravity contribution is incorporated in the pressure. All equations are written in a coordinate free form. The stress tensor obeys the following law for generalized Newtonian fluids

$$\boldsymbol{\tau} = 2\eta(\dot{\gamma})\mathbf{D} \tag{3}$$

with the rate of strain tensor $\mathbf{D}$ given by

$$\mathbf{D} = \frac{1}{2}([\nabla\mathbf{u}] + [\nabla\mathbf{u}]^{\mathsf{T}}), \tag{4}$$

and $\eta(\dot{\gamma})$ representing the fluid viscosity function.

Considering steady, incompressible, laminar flow (in the streamwise x direction) between two infinite parallel horizontal plates, with no movement in the y direction (Fig. 1), the momentum equation (Eq. (2)) written in a Cartesian coordinate system reduces to

$$\frac{d}{dy}\left(\eta(\dot{\gamma})\frac{du}{dy}\right) = p_x \tag{5}$$

where $p_x = dp/dx$. This equation is valid for both planar Couette and Poiseuille flow.

For fluids described by the Generalized Newtonian model, the empirical viscosity function $\eta(\dot{\gamma})$ can be given by any of the models in Eqs. (6)–(10). These are the power law model

$$\eta(\dot{\gamma}) = a|\dot{\gamma}|^{n-1} \tag{6}$$

and the Sisko model

$$\eta(\dot{\gamma}) = \mu_\infty + a|\dot{\gamma}|^{n-1}, \tag{7}$$

where $\dot{\gamma}$ is the shear rate obtained from the following definition involving the second invariant of the rate of deformation tensor ($|\dot{\gamma}| = \sqrt{D_{ij}D_{ij}/2}$) and a, n are the consistency and power law indices with $n \geq 0$, and μ_∞ is the viscosity at a very large shear rates.

Analytical solutions are also presented for yield stress fluids described by the following two models:

$$\text{Herschel--Bulkley model :} \quad \begin{cases} \boldsymbol{\tau} = 2\left(\mu_0|\dot{\gamma}|^{n-1} + \frac{\tau_0}{|\dot{\gamma}|}\right)\mathbf{D} & if\ |\tau| > \tau_0 \\ \mathbf{D} = 0 & if\ |\tau| \leqslant \tau_0 \end{cases} \tag{8}$$

$$\text{Robertson--Stiff model :} \quad \begin{cases} \boldsymbol{\tau} = \left(\mu_0^{1/n}|\dot{\gamma}|^{(n-1)/n} + \left(\frac{\tau_0}{|\dot{\gamma}|}\right)^{1/n}\right)^n\mathbf{D} & if\ |\tau| > \tau_0 \\ \mathbf{D} = 0 & if\ |\tau| \leqslant \tau_0 \end{cases} \tag{9}$$

where τ_0 is the yield stress and $\mu_0 \geqslant 0$. For $n = 1$ the Herschel–Bulkley model reduces to the Bingham model. For the yield stress models $|\tau|$ is the second invariant of the deviatoric stress tensor $|\tau| = \sqrt{\tau_{ij}\tau_{ij}/2}$.

2.2. Boundary conditions

The specification of boundary conditions is mandatory to guarantee the wellposedness of the problem. As mentioned before, most solutions in the literature are for the Dirichlet type no-slip wall boundary condition

$$\mathbf{u} = \mathbf{0}. \tag{10}$$

This imposes that the fluid adheres to the wall, together with the impermeability condition.

However, this boundary condition cannot be derived from first principles [4]. Lamb [21], Batchelor [22] and Goldstein [23] mention that slip may be wrong and that the use of no-slip stems from the need to agree predictions with experiments (some of the experiments referred to were not carried out carefully and consequently their results are contradictory). Several authors [4] try to explain the existence of slip and its dependence on parameters like surface roughness, dissolved gas and bubbles attached to the wall, wetting characteristics, shear rate, electrical properties and pressure, and this list keeps increasing with time.

In any case it is now an established fact that for macro geometries the interaction between small fluid molecules and walls is equivalent to a no-slip condition for most fluid-wall pairs. However, as the Knudsen number (the ratio between the mean free
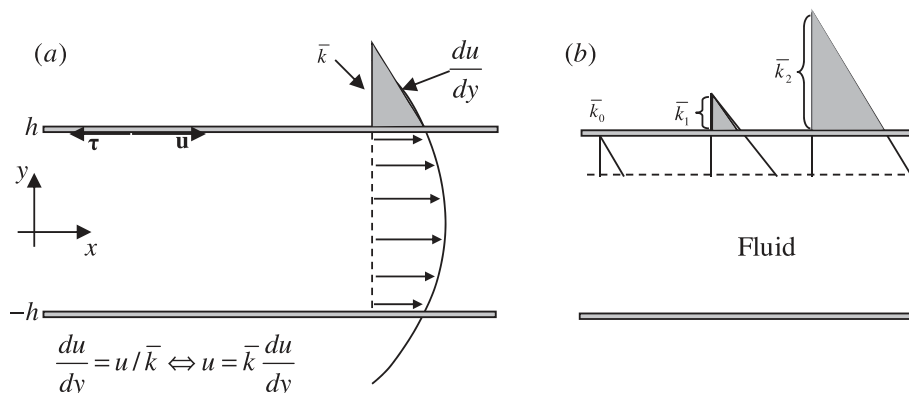

Fig. 1. (a) Velocity profile across the flow channel assuming Couette–Poiseuille flow and slip at the wall (b) Different slip lengths $0 = \bar{k}_0 < \bar{k}_1 < \bar{k}_2$ (zoom of the channel near the wall).

path and the characteristic flow size) increases, slip effects become more important ([4] and references cited therein). Regarding long molecules, such as the ones found in polymer melts, slip effects can actually be found also at the macro scale leading to some flow instabilities reviewed by Denn [1], such as sharkskin, stick–slip and gross melt fracture. Other investigations concerning slip at the liquid–solid interface for polymers are Potente et al. [7] and Mitsoulis et al. [24].

2.3. Slip laws

Friction between a fluid in contact with a wall generates a tangent stress vector τ (Fig. 1) that may be sufficient to eliminate slip of the fluid. Therefore, a way to promote slip is to reduce that friction, leading to the appearance of a nonzero velocity along the wall. The tangent stress vector depends on the velocity gradient of the fluid at the wall, with both variables related in such a way that the tangent velocity and tangent stress vectors are pointing in opposite directions (Fig. 1).

Since all the analytical solutions in this work concern flow between parallel plates aligned with the axis x direction, there is no need to continue using vector notation, so, all the slip laws will be presented in their streamwise component.

Navier [25] argued that in the presence of slip the liquid motion must be opposed by a force proportional to the relative velocity between the first liquid layer and the solid wall. Fig. 1 illustrates an interpretation of slip with Fig. 1a showing the velocity profile across the channel and the relation between the velocity and its derivative at the wall. This derivative at the wall is the same as the slope given by $u/\bar{k}$. Thus, the following relation that involves the slip velocity can be obtained

$$\frac{u_{ws}}{\bar{k}} = \frac{du}{dy}\bigg|_{wall}. \tag{11}$$

Solving for u_{ws}, the relationship between the slip velocity and the wall velocity gradient is

$$u_{ws} = \bar{k}\frac{du}{dy}\bigg|_{wall}, \tag{12}$$

where the coefficient $\bar{k}$ is named slip length or friction coefficient. As illustrated in Fig. 1b the slip length can take any positive value ($\bar{k} \geqslant 0$), with no-slip at wall for $\bar{k} = 0$, and increasingly large slip velocity as $\bar{k}$ increases to infinity in which case the velocity profile becomes a plug with zero velocity gradient.

Eq. (12) must be combined with the rheological constitutive equation. Considering the Generalized Newtonian Fluid model for inelastic fluids, near the wall the tangent stress is given by

$$\tau_{xy} = \eta(\dot{\gamma})\frac{du}{dy} \tag{13}$$

Eq. (12) can now be rewritten for a Generalized Newtonian fluid as

$$u_{ws} = sign(du/dy)k\tau_{xy} \tag{14}$$

with $k = \bar{k}/\eta(\dot{\gamma}) \geqslant 0$. Based on the fact that the velocity points to the stress opposite direction and because scalar variables are employed, different signs will be used in Eq. (14) depending on the sign of the shear rate ($sign(du/dy)$). For the "top wall", the equation makes use of the minus sign and for the "bottom wall" the plus sign, since the tangent velocity is positive in both walls but the $sign(du/dy)$ in the top and bottom walls is negative and positive, respectively. This notation will stand for the other slip laws.

This linear relationship between slip velocity at the wall u_{ws} and shear stress at the wall τ_{xy} is called the **linear Navier slip law** [25] or simply the **Navier slip law**. It has been used extensively to rep-

resent experimental data, as in [5–7,10] for Couette and Poiseuille flows.

Slip laws are models to bridge the gap between theory and experimental data, and to fit experimental observations various slip models were created, such as those stating the dependence of the friction coefficient on wall shear rate or stress and models derived from molecular kinetic theory [26–28].

The **non-linear Navier slip law** [26] assumes that the friction coefficient is a function of the shear stress τ_{xy}, thus providing a non-linear power function,

$$u_{ws} = sign(du/dy)k|\tau_{xy}|^{m-1}\tau_{xy} \tag{15}$$

where $m > 0 (m \in \mathbb{R})$. For $m = 1$ the Navier slip law is recovered.

This non-linear model has been used to represent experimental data in Couette and Poiseuille flows by [13,23,26]. It provides a good approximation for several conditions, but it fails to describe the slip velocity in the neighborhood of the critical stress at which the slip starts [27]. To eliminate this discrepancy, Hatzikiriakos proposed an alternative slip law based on the Eyring theory of liquid viscosity in order to provide a smooth transition from no-slip to slip flow at the critical shear stress [27]. The argument goes as follows:

Let τ_c be the positive critical stress at which slip starts and k_1, $k_2 \geqslant 0$. Then, the **Hatzikiriakos slip law** is given by,

$$u_{ws} = \begin{cases} k_1 \sinh(k_2(sign(du/dy)\tau_{xy}) - \tau_c) & if \ \tau_{xy} \geq \tau_c \\ 0 & if \ \tau_{xy} < \tau_c \end{cases} \tag{16}$$

The **asymptotic slip law** [28], is given by

$$\tau = -(1/k_2), [1 - \exp(u/k_1)] \tag{17}$$

for one dimensional flow, and can also be written as an explicit function for the slip velocity

$$u_{ws} = k_1 \ln(1 + k_2 (sign(du/dy)\tau_{xy})). \tag{18}$$

For both the Hatzikiriakos and the asymptotic slip models, the coefficients k_1 and k_2 allow controlling the amount of slip and the shape of the curve of $\tau \ vs \ u_{ws}$ that is obtained by experimental measurements. Schowalter [26] used the Hatzikiriakos slip law model to model wall slip in Couette and Poiseuille flows.

For the Poiseuille and Couette flows of Figs. 1 and 2 the boundary conditions for these slip laws can be written in a general form for both the "top" ($+h$) and "bottom" ($-h$) walls.

Integrating the momentum equation (Eq. (5)) τ_{xy} is given by

$$\tau_{xy} = p_x y + c. \tag{19}$$

Combining Eq. (19) with Eqs. (15), (16), and (18) for all the investigated slip laws gives the general form of the boundary conditions at the upper and bottom walls.

For the non-linear Navier slip law ($m = 1$ for the linear Navier slip law):

$$u(h) = k_{nl1}(-p_x h - c)^m. \tag{20-a}$$

$$u(-h) = k_{nl2}(-p_x h + c)^m. \tag{20-b}$$

For the Hatzikiriakos slip law:

$$u(h) = k_{H1} \sinh(k_{H2}(-p_x h - c)). \tag{21-a}$$

$$u(-h) = k_{H3} \sinh(k_{H4}(-p_x h + c)). \tag{21-b}$$

For the asymptotic slip law:

$$u(h) = k_{A1} \ln(1 + k_{A2}(-p_x h - c)). \tag{22-a}$$

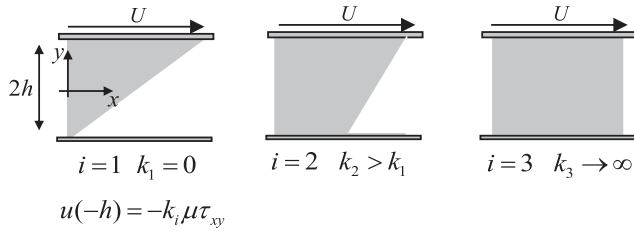$$u(-h) = k_{A3} \ln(1 + k_{A4}(-p_x h + c)). \tag{22-b}$$

Fig. 2. Couette flow velocity profiles for different slip lengths $k_1 < k_2 < k_3$..

For symmetrical boundary conditions $c_1 = 0$, thus the top and bottom slip velocities become identical, as expected.

3. Analytic and semi analytic solutions for Newtonian fluids

Newtonian fluids have a constant viscosity so $\eta(\dot{\gamma}) = \mu$ in Eq. (13).

3.1. Couette flow

In pure Couette flow (Fig. 2) the pressure gradient is null and Eq. (5) reduces to:

$$u(y) = c_1 y + c_2 \tag{23}$$

with c_1 the shear rate $\dot{\gamma} = du/dy$.

3.1.1. Navier slip at the bottom wall and no slip at the upper wall

Assume the upper wall is moving with velocity U and that a Navier slip boundary condition applies to the bottom wall (cf. Fig. 2) so that

$$u(h) = U \text{ and } u(-h) = k\mu\left(\frac{du}{dy}\right)_{y=h} = k\mu c_1 \tag{24}$$

Using the boundary condition of Eq. (24) the coefficients c_1 and c_2 are given by

$$c_2 = U - c_1 h, \tag{25}$$

$$c_1 = \frac{U}{2h + k\mu}. \tag{26}$$

The final solution for the velocity profile across the channel is then

$$u(y) = \frac{U(y - h)}{2h + k\mu} + U. \tag{27}$$

Let $f(k)$ be defined by

$$f(k) = \frac{U(y - h)}{2h + k\mu} + U \ , k \geqslant 0. \tag{28}$$

For $k = 0$, $f(0) = (U/2h)(y + h)$ which is the original solution with the Dirichlet boundary condition $u = 0$. As k increases the solution approaches plug flow conditions, i.e.

$$\lim_{k\to\infty} f(k) = \lim_{k\to\infty} \frac{U(y - h)}{2h + k\mu} + U = U \tag{29}$$

This equation states that it is impossible to obtain a slip velocity larger than U, which is in agreement with the physical constraints of the problem. Fig. 2 illustrates the evolution of the flow with the slip length.

If $U = 0$ the flow profile is given by the trivial solution $u(y) = 0$ for $0 \leqslant y \leqslant h$. The main problem with this slip boundary condition (Eq. (24)) is that both the bulk and wall velocities depend on the velocity gradient, so that a nonzero gradient will develop only if

some velocity is given at the boundary. Therefore, it can be said that the Navier slip boundary condition is somewhat weaker than the Dirichlet boundary condition, so that in the absence of a pressure gradient and of an imposed velocity the fluid will not move. Note that for $U = 0$ and imposing slip at both walls leads again to the trivial solution $u(y) = 0$.

3.1.2. Non-linear slip laws at the bottom wall and no slip at the upper wall

Assume the upper wall is moving with velocity $u(h) = U$ and a non-linear slip boundary condition is imposed at the bottom wall. Following a procedure similar to that of the previous section the following boundary conditions are obtained: for the non-linear Navier slip law $u(-h) = k_{nl2}(\mu c_1)^m$, for the Hatzikiriakos slip law $u(-h) = k_{H3} \sinh(k_{H4}\mu c_1)$ and for the asymptotic slip law $u(-h) = k_{A3} \ln(1 + k_{A4}\mu c_1)$.

To determine the integration constant c_1, the following equations must be solved for the non-linear Navier slip law, Hatzikiriakos and asymptotic slip laws, respectively

$$(c_1)^m + (2h/k\mu^m)c_1 - (U/k\mu^m) = 0 \tag{30-a}$$

$$k_{H3} \sinh(k_{H4}\mu c_1) + 2hc_1 - U = 0 \tag{30-b}$$

$$k_{A3} \ln(1 + k_{A4}\mu c_1) + 2hc_1 - U = 0 \tag{30-c}$$

For the special cases of $m = 0.5, 2, 3$ the analytical solutions are possible for the non-linear Navier slip law, the results of which are presented in Table 1 and Appendix A. For the other solutions and equations we prove the existence of a unique solution in Appendix A.

3.2. Couette–Poiseuille flow

Integrating twice the momentum equation (Eq. (5)) for a constant viscosity fluid, the result is

$$u(y) = \frac{p_x}{2\mu}y^2 + c_1 y + c_2 \tag{31}$$

with $c_1 = c/\mu, c_2 \in \mathbb{R}$ two real constant numbers, $\mu \geqslant 0$ and $-h \leqslant y \leqslant h$. Applying boundary conditions $u(-h)$ and $u(h)$ to the velocity profile in Eq. (31) the constants of integration c_1, c_2 can be determined and the following final form of the velocity profile is obtained

$$u(y) = \frac{p_x}{2\mu}(y^2 - h^2) + \left(\frac{u(h) - u(-h)}{2h}\right)y + \frac{u(-h) + u(h)}{2} \tag{32}$$

For the particular case of pure Poiseuille flow, symmetry leads to $c_1 = 0$ and $c_2 = u(h) - (p_x/2\eta(\dot{\gamma}))h^2$.

For the inverse problem of Couette–Poiseuille flow with an imposed flow rate $Q = \overline{U} \cdot 2h$, where $\overline{U}$ is the mean velocity obtained by integration of the velocity profile across the channel, we obtain the relation of Eq. (33) between the imposed mean velocity and the ensuing pressure gradient

$$\overline{U} = \frac{1}{2h} \int_{-h}^{h} \left(\frac{p_x}{2\mu}y^2 + c_1 y + c_2\right) dy$$

$$\iff -\frac{p_x}{3\mu}h^2 + \frac{u(-h) + u(h)}{2} - \overline{U} = 0 \tag{33}$$

Notice that $u(-h)$ and $u(h)$ are themselves functions of the pressure gradient, and non-linear equations may arise.

3.2.1. Linear and non-linear slip laws – pure Poiseuille flow

For the linear and non-linear slip models and from the boundary conditions of Eqs. (20-a), (21-a) and (22-a) the flow velocity profile for the direct problem becomes

Table 1

Analytical solutions for Couette flow with linear and non-linear Navier slip laws and slip only at the bottom wall. The top row shows the general system of equations to be solved and the next four rows show the solution for different values of the slip exponent $m = 0.5, 1, 2, 3$.

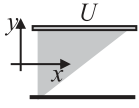|	
Couette flow [linear (m = 1) and non-linear Navier slip (m ≠ 1)]	$\begin{cases} u(y) = c_1(y-h) + U \\ (c_1)^m + (2h/k\mu^m)c_1 - (U/k\mu^m) = 0 \end{cases}$
	$m = 0.5 \quad u(y) = \left[\frac{(k\mu^{0.5})^2}{8h^2}\left(1 - \sqrt{1 + \frac{8hU}{(k\mu^{0.5})^2}}\right) + \frac{U}{2h}\right](y-h) + U$
	$m = 1 \quad u(y) = \frac{U(y-h)}{2h + k\mu} + U$
	$m = 2 \quad u(y) = \frac{-2h + \sqrt{4(h^2 + k\mu^m U)}}{2k\mu^m}(y-h) + U$
	$m = 3 \quad u(y) = \left\{\sqrt[3]{(U/k\mu^m)/2 + \sqrt{((U/k\mu^m)/2)^2 + ((2h/k\mu^m)/3)^3}} + \sqrt[3]{(U/k\mu^m)/2 - \sqrt{((U/k\mu^m)/2)^2 + ((2h/k\mu^m)/3)^3}}\right\}(y-h) + U$

Table 2

Analytical solutions for Poiseuille flow with identical slip at both walls for the linear and non-linear Navier slip laws. In the top row the general system of equations to be solved and the next four rows show the solution for different values of the slip exponent $m = 0.5, 1, 2, 3$.

Poiseuille flow [linear (m = 1) and non-linear Navier slip (m ≠ 1)]	$\begin{cases} u(y) = \frac{p_x}{2\mu}(y^2 - h^2) + kh^m(-p_x)^m \\ -\frac{p_x}{3\mu}h^2 + kh^m(-p_x)^m - \overline{U} = 0 \end{cases}$
	$m = 0.5 \quad p_x = \frac{-9\mu^2}{4h^4}\left(2k^2h + \frac{4h^2\overline{U}}{3\mu} - 2kh^{0.5}\sqrt{k^2h + \frac{4h^2\overline{U}}{3\mu}}\right)$
	$m = 1 \quad p_x = \overline{U}(-h^2/3\mu - kh)^{-1}$
	$m = 2 \quad p_x = \frac{h^2/3\mu \pm \sqrt{(h^2/3\mu)^2 + 4kh^2\overline{U}}}{2kh^2}$
	$m = 3 \quad p_x = \left(\sqrt[3]{-(\overline{U}/2kh^3) + \sqrt{(\overline{U}/2kh^3)^2 + (9kh\mu)^{-3}}} + \sqrt[3]{-(\overline{U}/2kh^3) - \sqrt{(\overline{U}/2kh^3)^2 + (9kh\mu)^{-3}}}\right)$
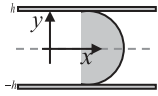
$$u(y) = \frac{p_x}{2\mu}(y^2 - h^2) + u(h), \qquad (34)$$

whereas for the inverse problem the pressure gradient is obtained from the following transcendent equation for a given bulk velocity $\overline{U}$

$$-\frac{p_x}{3\mu}h^2 + u(h) - \overline{U} = 0. \qquad (35)$$

Generally speaking the solution of the previous equation must be obtained numerically, but for the particular cases of the non-linear Navier slip law with $m = 0.5$, $m = 1$ (linear), $m = 2$ and $m = 3$ full analytical solutions can be obtained and are given in Table 2. For the Hatzikiriakos and asymptotic slip laws, the corresponding solutions are presented in Table 3. Details on these solutions are given in Appendix B, where the existence of a unique solution for all the boundary conditions is also proved.

Note that the solution of Hatzikiriakos and Mitsoulis [29] is less general. Even though they investigated a power law fluid with non-linear Navier slip boundary conditions, they restricted their solutions to the particular case $m = 1/n$, where n is the power law exponent, meaning that for the Newtonian case they only explore the linear Navier slip.

3.2.2. Different slip in the upper and bottom walls for Couette-Poiseuille flow

When compared to the pure Poiseuille flow we see that for the Couette-Poiseuille flow the symmetry condition ($c_1 = 0$) can no longer be used, meaning that, a system of non-linear equations will be obtained for the constant of integration c_1 and the pressure gradient p_x (Eq. (36))

$$\begin{cases} -2hc_1 + u(h) - u(-h) = 0 \\ -\frac{p_x}{3\mu}h^2 - c_1h + u(h) - U = 0 \end{cases}. \qquad (36)$$

For the **linear Navier slip law** at both walls (with slip coefficients k_{l1} at the bottom and k_{l2} at the top), the analytical solution is still possible and is given by Eq. (37)

$$u(y) = \frac{p_x}{2\mu}y^2 + c_1y + p_x\left(-k_1h - \frac{h^2}{2\mu}\right) + c_1(-k_1\mu - h). \qquad (37)$$

with

$$p_x = -\frac{3/2(2 + k_{l1}(\mu U/h) + k_{l2}(\mu U/h))}{[3k_{l1}(\mu U/h)k_{l2}(\mu U/h) + 2k_{l1}(\mu U/h) + 2k_{l2}(\mu U/h) + 1](\mu U/h^2)}, \qquad (38)$$

$$c_1 = \frac{3/2U(\mu U/h)(k_{l1} - k_{l2})}{[3k_{l1}(\mu U/h)k_{l2}(\mu U/h) + 2k_{l1}(\mu U/h) + 2k_{l2}(\mu U/h) + 1]h}. \qquad (39)$$

For this case, the boundary conditions are given by Eqs. (20-a) and (20-b) with $m = 1$. The term $(k_{l1} - k_{l2})$ will determine the sign of c_1. If $k_{l1} > k_{l2}$ the maximum velocity value is on the positive half of the channel $0 \leqslant y \leqslant h$ whereas for $k_{l1} < k_{l2}$ it is on the lower half $-h \leqslant y \leqslant 0$.
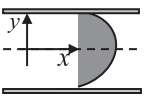
For **the non-linear Navier slip law**, full analytical solutions can also be found, when the linear Navier slip law is valid in one wall, and on the other the non-linear Navier slip law applies with m equal to 2 or 3. These solutions can be very helpful to test numerical codes with different slip boundary conditions in the same domain, and can be found in Appendix C.

For the remaining values of the exponent and for the other two slip models (asymptotic and Hatzikiriakos), semi-analytical solutions are obtained. Their restrictions, $du/dy < 0$ in the upper wall, $du/dy > 0$ in the bottom wall, and a favorable pressure gradient ($p_x < 0$), are helpful to narrow down the possible solutions, especially when the use of a numerical method is required.

Table 3
Semi-analytical solutions for the Poiseuille flow of a Newtonian fluid with Hatzikiriakos and asymptotic slip laws.

Poiseuille flow [Hatzikiriakos and asymptotic]		$\begin{cases} u(y) = \frac{p_x}{2\mu}(y^2 - h^2) + u(h) \\ -\frac{p_x}{3\mu}h^2 + u(h) - \overline{U} = 0 \end{cases}$

Table 4
Analytical solutions for Couette–Poiseuille flow with different slip coefficients at the top and bottom walls, as a function of p_x and c_1. The third row presents the equations that need to be solved to determine p_x and c_1 for the non-linear slip models.

Poiseuille flow [different slip at top and bottom walls]

$$u(y) = \frac{p_x}{2\mu}y^2 + c_1 y + p_x\left(-k_1 h - \frac{h^2}{2\mu}\right) + c_1(-k_1\mu - h)$$

$$p_x = -\frac{1.5(2 + k_1(\mu\overline{U}/h) + k_2(\mu\overline{U}/h))}{[3k_1(\mu\overline{U}/h)k_2(\mu\overline{U}/h) + 2k_1(\mu\overline{U}/h) + 2k_2(\mu\overline{U}/h) + 1](\mu\overline{U}/h^2)}$$

$$c_1 = \frac{1.5U(\mu\overline{U}/h)(k_1 - k_2)}{[3k_1(\mu\overline{U}/h)k_2(\mu\overline{U}/h) + 2k_1(\mu\overline{U}/h) + 2k_2(\mu\overline{U}/h) + 1]h}$$

$$\begin{cases} -2hc_1 + u(h) - u(-h) = 0 \\ -\frac{p_x}{3\mu}h^2 - c_1 h + u(h) - U = 0 \end{cases}$$

Non-linear Navier slip	Hatzikiriakos	Asymptotic
$u(h) = k_1(-p_x h - \mu c_1)^m$	$u(h) = k_1 \sinh(k_2(-p_x h - \mu c_1))$	$u(h) = k_1 \ln(1 + k_2(-p_x h - \mu c_1))$
$u(-h) = k_2(-p_x h + \mu c_1)^m$	$u(-h) = k_3 \sinh(k_4(-p_x h + \mu c_1))$	$u(-h) = k_3 \ln(1 + k_4(-p_x h + \mu c_1))$

$p_x < 0$ and $\underbrace{-p_x h - \mu c_1 > 0 \text{ and } -p_x h + \mu c_1 > 0}_{\text{the slip velocity points in the positive direction}}$

$$\Longleftrightarrow p_x < 0 \text{ and } c_1 \in \left]\frac{p_x}{\mu}h - \frac{p_x}{\mu}h\right[\tag{40}$$

See Table 4 for a summary of these solutions.

3.3. Discussion (Newtonian fluids)

All the solutions obtained for the Newtonian fluids are summarized in Tables 1–4, which will be used for the subsequent discussion. In Poiseuille flow the following dimensionless variables will be used. The slip friction coefficients are given by $k'_{nl} = k\overline{U}^{m-1}(\mu/h)^m$ for the Navier non-linear slip model, $k'_1 = k_1/\overline{U}$, $k'_2 = k_2(\mu\overline{U}/h)$, for the first and second coefficients in the asymptotic and Hatzikiriakos slip laws. The velocity is given by $u' = u/\overline{U}$ and the pressure gradient by $p'_x = p_x/(\eta\overline{U}/h^2)$.

3.3.1. Couette flow

For the Couette flow several flow conditions were studied. Fig. 3 shows the influence of the non-linear Navier slip model exponent (m) on the velocity profile for different values of the friction coefficient (k'_{nl}). The slip velocity decreases inversely to exponent m, so it becomes increasingly difficult to attain the plug flow conditions when m increases.

This behavior can be also verified by variation of the shear rate $c_1 = du/dy$ with the slip coefficient, seen in Fig. 4. As shown for the case with exponent $m = 2$, du/dy is larger than for the $m = 1$ case. Notice that du/dy will multiply a negative number (see Table 1), thus reducing the slip velocity for higher slip exponents.

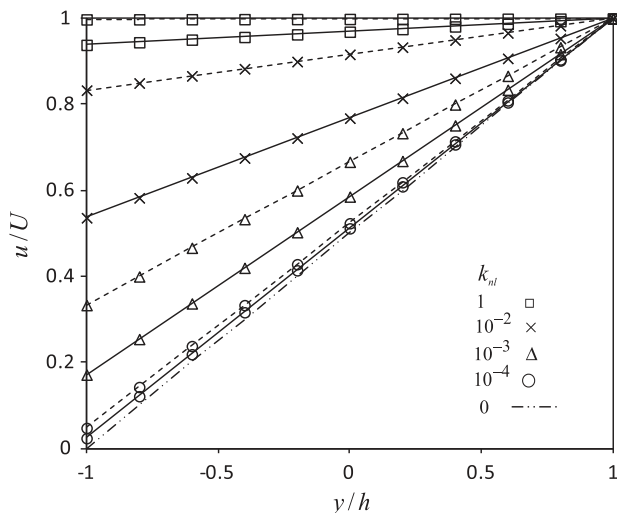**Fig. 3.** Velocity profiles for the Couette flow with the non-linear Navier slip model (full line $m = 2$, dashed line $m = 1$) at the fixed wall.
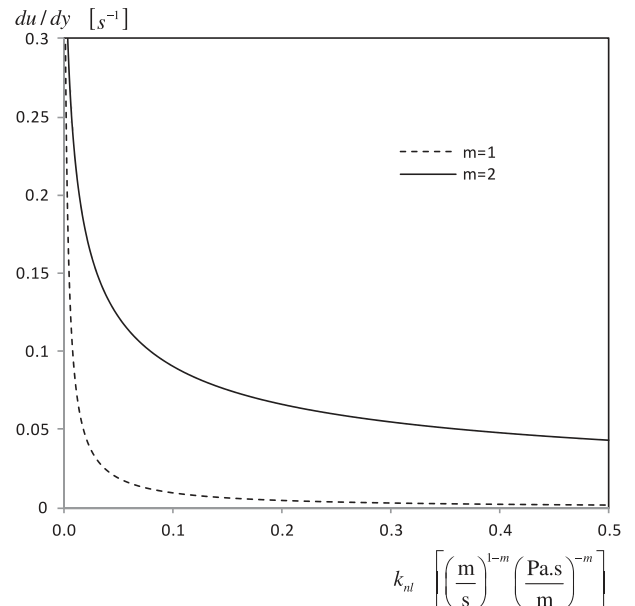

Fig. 4. Integral constant c_1 versus the friction coefficient for the Couettte flow with non-linear Navier slip model at the fixed wall.

Fig. 6. Variation of the normalized pressure gradient (a) and slip velocity (b) with the dimensionless slip coefficient k'_{nl} for different values of the slip exponent m for Poiseuille flow in a channel.
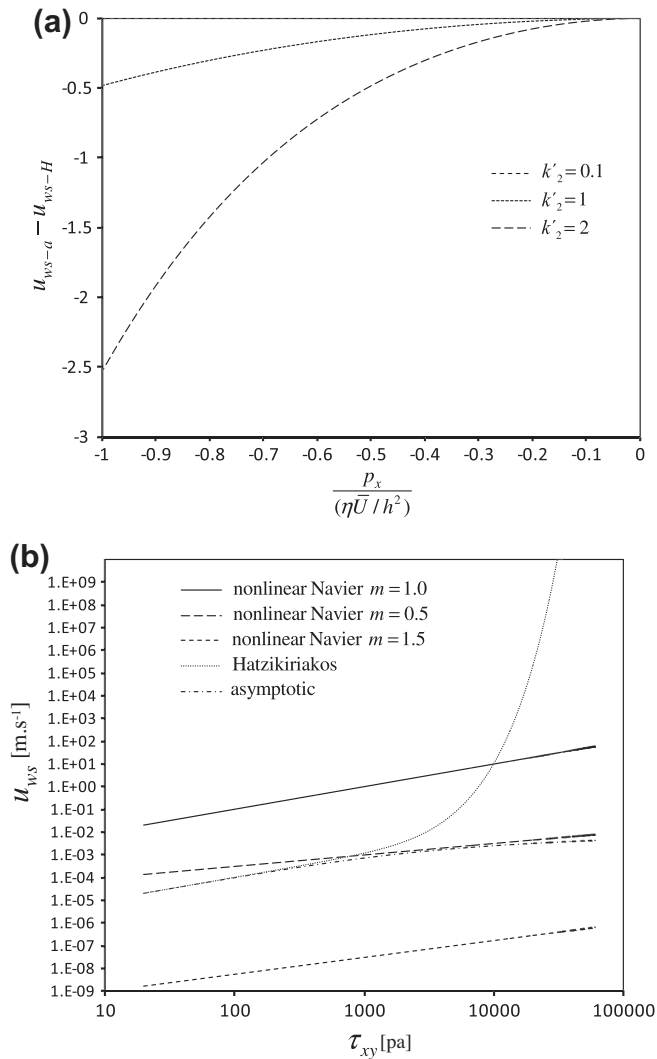
Fig. 5. (a) Difference between the asymptotic (A) and the Hatzikiriakos (H) slip velocities for different values of the dimensionless slip coefficient k'_2. It is assumed that $k'_1 = 1$. (b) Representation of the four slip boundary conditions (slip velocity versus shear stress) for equal and constant friction coefficients.

3.3.2. Poiseuille flow (symmetrical conditions)

In Fig. 5a the difference in slip velocity between the asymptotic and Hatzikiriakos slip laws is illustrated. For different values of the slip coefficient k'_2 the sensitivity of the models is different. Notice that the Hatzikiriakos slip law is built with the inverse function of the asymptotic law, and therefore its growth is exponential. For small values of k'_2 both functions tend to a linear "local" behavior for some specific range of the pressure gradient, and for these values they locally have a similar behavior as can be seen in Fig. 5.

The Hatzikiriakos slip law is much more sensitive to the k'_2 coefficient than the asymptotic slip law, as can be seen in Fig. 5b. This fact can be a problem when implementing this law in numerical codes, mainly due to convergence difficulties, since along the iterative procedure large variations in the slip velocity can occur and cause divergence (overflow) or even round off errors on the final data.

The other slip parameter k'_1 increases or decreases the slip velocity establishing a linear relationship between the slip velocity and the hyperbolic sine or logarithmic functions.

In Fig. 5b we can also see the agreement between the Hatzikiriakos and asymptotic slip laws for lower values of the shear stress. Notice the almost linear growth of the slip velocity for the nonlinear Navier slip laws, while the Hatzikiriakos slip law has a sigmoid shape with an inflection point, where the curvature changes
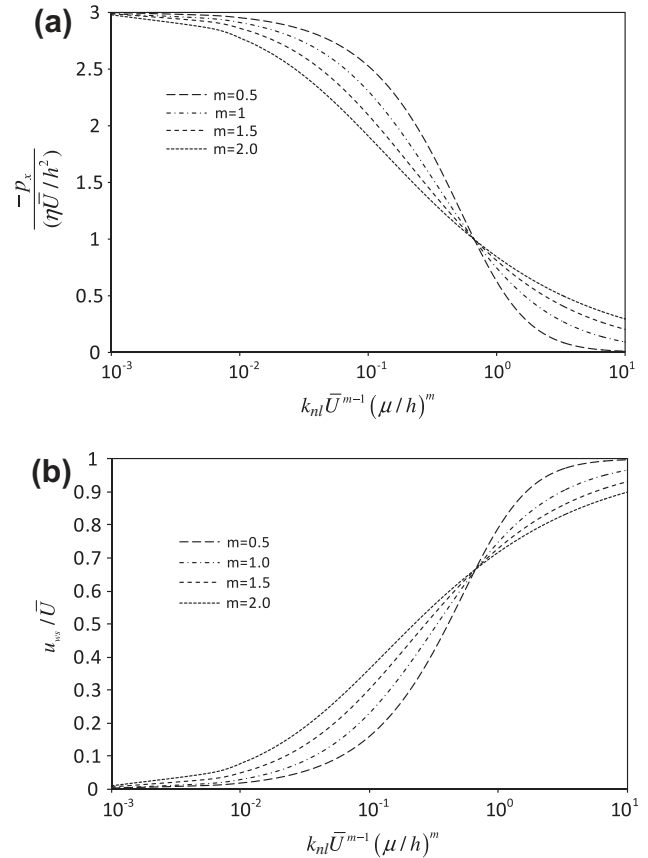
(in Fig. 5b the complete sigmoid shape cannot be seen because we use null critical stress).

The slip intensity influences the pressure gradient, which promotes the fluid flow. As the resistance of the walls decrease a smaller pressure gradient is enough to ensure motion as shown in Fig. 6a, where the variation of the pressure gradient with the slip coefficient is represented. These effects can also be analyzed in terms of the dimensionless slip velocity, shown in Fig. 6b, where similar trends to those obtained for pressure gradient are depicted.

It should be noticed that with dimensionless variables the slip coefficient k'_{nl} depends on the slip exponent which may influence the results, since the coefficient is different for each flow exponent (m). However, plotting the data in nondimensional form shows the same qualitative behavior.

For the Hatzikiriakos and asymptotic slip models, the behavior is slightly different when compared with the Navier slip model as shown in Fig. 7. For the slip constant $k'_1 = 1$, both models exhibit the same qualitative behavior as is also the case for the Navier Slip model. However, as the coefficient k'_1 decreases, their behavior departs from each other and from the Navier slip.

The asymptotic model is greatly influenced by the slip coefficient k'_1 showing a nearly constant pressure gradient which slowly decreases with slip, whereas the slip velocity increases strongly with the slip coefficient k'_2.

The Hatzikiriakos model results in smaller pressure gradient and higher slip velocities than the asymptotic model for the same numerical value of the slip coefficients. As seen in Fig. 7, the trend in the slip velocity for the $k'_1 = 10^{-3}$ (Hatzikiriakos) is quite different from the other slip trend lines. At some point this model seems to be very sensitive to the friction coefficients and the slip velocity increases drastically, thus creating numerical instabilities.
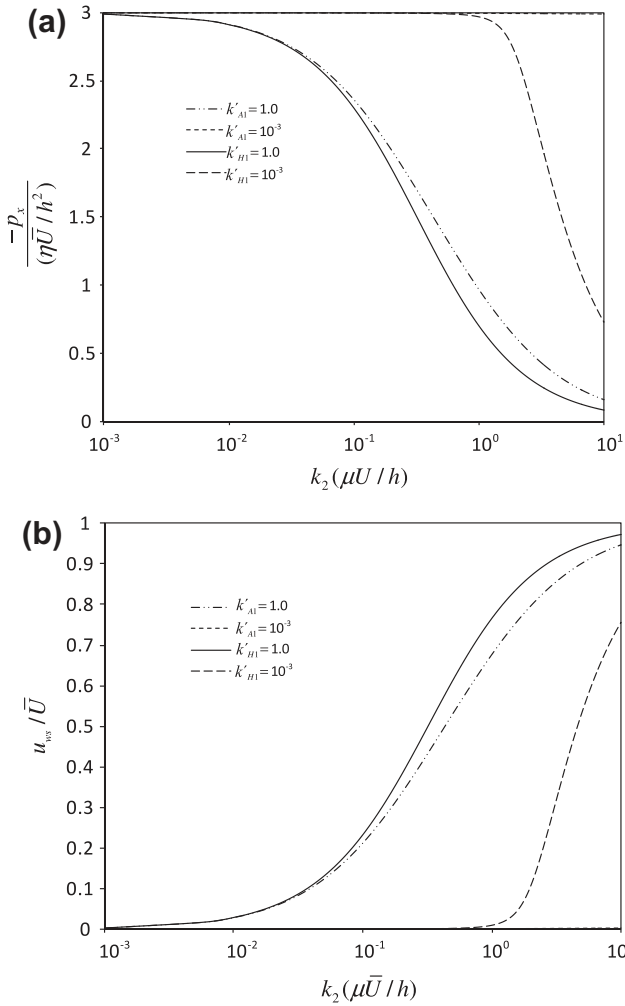
Fig. 7. Comparison between the asymptotic and Hatzikiriakos slip laws for Poiseuille flow in a channel. (a) Variation of the normalized pressure drop for different values of the slip coefficient k'_2 and two different values of k'_1. (b) Variation of the normalized slip velocity with the pressure drop.

3.3.3. Different slip in both walls

For the analysis of the different slip coefficients at both walls, the linear Navier slip boundary condition was chosen. The variation of the pressure gradient with k'_l is shown in Fig. 8a for a case with no slip at one boundary, showing that the normalized pressure gradient varies from -3 for $k'_l = 0$ to a maximum value of -0.75 for $k'_l \to \infty$. Different slip conditions distort the velocity profile as plotted in Fig. 8b. As the slip velocity increases the velocity peak tends to the wall, where there is slip ($y/h = -1$). Still in this particular case, it is easily proven that the velocity profile for the limiting condition of infinite friction coefficient is given by the following quadratic expression

$$\frac{u}{\overline{U}}(y) = 0.375\left[\left(\frac{y}{h}\right)^2 - 1\right] + \left[\frac{y}{h} - 1\right]. \tag{41}$$

4. Non-Newtonian fluids (Poiseuille flow)

4.1. Power law fluids

Analytical and semi-analytical solutions are derived for non-Newtonian fluids obeying the "power law" viscosity model. The solution for imposed pressure gradient flow (direct problem) in the extrusion barrel geometry given by Newtonian slip law has
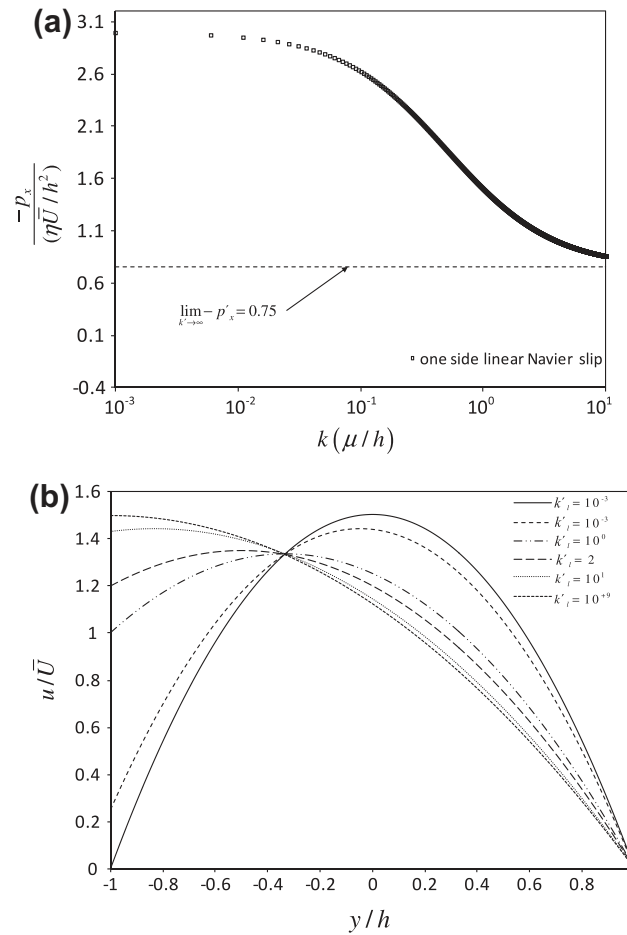
Fig. 8. Study of the linear Navier slip boundary condition applied to the bottom wall of a channel flow: (a) Variation of the pressure gradient with the friction coefficient. (b)Velocity profile with no slip velocity at the top wall ($y = 1$) and different slip coefficients at bottom ($y = -1$).

been reported elsewhere [6,8] and we look now at the inverse solution.

Consider the momentum equation (Eq. (5)), with the variable viscosity of Eq. (6). For symmetric boundary conditions consider only the lower half channel, where the velocity gradient is positive

$$\eta(\dot{\gamma}) = a\left(\frac{du}{dy}\right)^{n-1} \tag{42}$$

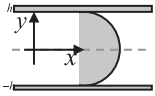For wall slip $u(-h)$ the velocity profile is given by (cf. [30] for the pipe flow case)

$$u(y) = \left(\frac{-p_x}{a}\right)^{1/n}\left(\frac{h^{(1/n)+1}}{(1/n)+1} - \frac{(-y)^{(1/n)+1}}{(1/n)+1}\right) + u(-h). \tag{43}$$

The solution for the "inverse problem" with an imposed mean velocity $\overline{U}$ is given by solving Eq. (44)

$$\left(\frac{-p_x}{a}\right)^{1/n}\left[\frac{h^{(1/n)+1}}{(1/n)+2}\right] + u(-h) - \overline{U} = 0 \tag{44}$$

Hatzikiriakos and Mitsoulis [29] studied these flows with Navier non-linear slip law for special cases of the slip exponents $1/n = m$ and making use of lubrication theory in tapered dies. They only presented full analytical solutions for the direct problem, whereas for the inverse problem the solutions are approximate because there is an unsolved integral in the equations. However, there is a closed

Table 5
Analytical solutions for Poiseuille flow of a power law fluid for different sets of power law (n) and slip (m) coefficients. nm.

Poiseuille flow: power-law fluid [linear (m = 1) and non-linear Navier slip ($m \neq 1$)]	$n = 0.5$ $m = 1$	$p_x = \frac{k_{nl}h^m - (k_{nl}h^m + 4\overline{U}[a^{-2}h^{(1/n)+1}(1/n+2)^{-1}])^{0.5}}{2[a^{-2}h^{(1/n)+1}(1/n+2)^{-1}]}$
	$n = 0.5$ $m = 2$	$p_x = -(\overline{U}/([h^{(1/n)+1}((1/n+2)a^2)^{-1}] + k_{nl}h^m))^{05}$
	$n = 0.5$ $m = 3$	Method given in a Appendix C
	$n = 1/3$ $m = 1$	$p_x = 3\sqrt{-q/2 + \sqrt{(q/2)^2 + (p/3)^2}} + 3\sqrt{-q/2 - \sqrt{(q/2)62 + (p/3)^2}}$
		$p = \frac{k_{nl}h}{[a^{-3}h^{(1/n)+1}(1/n+2)^{-1}]}$　　$q = \frac{\overline{U}}{[a^{-3}h^{(1+n)+1}(1/n+2)^{-1}]}$
	$n = 1/3$ $m = 2$	Method given in Appendix C
	$n = 1/3$ $m = 3$	$p_x = -\left(\overline{U}/([h^{(1/n)=1}((1/n+2)a^3)^{-1}]k_{nl}h^m)\right)^{1/3}$
	$n = 2$ $m = 1$	$p_x == \left(\frac{-L+(L^2+4\overline{U}L)^{0.5}}{2L}\right)^2$　　$L = [a^{-0.5}h^{(1/n)+1}(1/n+2)^{-1}]$

form solution for their special case "power-law ($n = 1/2$) with linear slip" which we give at the end of Appendix D.

For our geometry (Poiseuille flow in a channel), the analytical solutions for the special cases $n = 1/2$ with $m = 1, 2, 3$, $n = 1/3$ with $m = 1, 2, 3$ and $n = 2$ with $m = 1$ are also in closed form and given in Table 5. For other values of the slip exponents and other slip laws Appendix D includes the proof of existence of a unique solution.

4.2. Sisko model-particular solutions for n = 0.5 and n = 2

When the fluid viscosity obeys the Sisko model (Eq. (7)), integration of the momentum equation gives

$$\mu_\infty \frac{du}{dy} + a\left(\frac{du}{dy}\right)^n - p_x y = 0 \tag{45}$$

The solution of Eq. (45) is complex and is only given below (in closed form for the direct problem) for the cases $n = 0.5, 2$ (see Appendix E for the details).

For $n = 0.5$:

$$u(y) = \frac{\mu_\infty}{2a}(-y-h) + \frac{[(\mu_\infty)^2 + [4ap_x]y]^{3/2} - [(\mu_\infty)^2 - [4ap_x]h]^{3/2}}{12a^2 p_x} + u(-h) \tag{46}$$

For $n = 2$:

$$u(y) = \frac{a^2(y+h)}{2\mu_\infty^2} + \frac{p_x(y^2 - h^2)}{2\mu_\infty}$$
$$+ \frac{a([a^2 - [4\mu_\infty p_x]h]^{3/2} - [a^2 + [4\mu_\infty p_x]y]^{3/2})}{12\mu_\infty^3 p_x} + u(-h) \tag{47}$$

4.3. Discussion (non-Newtonian fluids)

Fig. 9a and b show the variations of pressure gradient and the slip velocity with the slip coefficient for both shear-thinning ($n < 1$) and shear-thickening ($n > 1$) fluids.

Increasing the slip coefficient decreases the magnitude of the favorable pressure gradient, with shear-thickening fluids leading to higher frictional loss than with shear-thinning fluids. Similar variations are observed for the slip velocity in Fig. 9b, except that for slip coefficients in excess of about 5×10^{-1}, where shear-thinning fluids have higher velocities than shear-thickening fluids.

For the non-linear Navier slip law, the viscosity power-law exponent has the major influence on the pressure gradient as seen in Fig. 10a, something that is confirmed also by Fig. 11b, for the Hatzikiriakos and asymptotic slip models. Fig. 10b also shows that the asymptotic model is much less sensitive to the friction coefficient than the Hatzikiriakos model.

4.4. Yield Stress fluids – Herschel–Bulkley and Robertson–Stiff models

The Poiseuille flow of a yield stress fluid is characterized by a "plug region" everywhere the yield stress τ_0 is not exceeded and, where the rate of strain tensor is identically zero.

The motion of the plug region Ω, is determined by the following form of the momentum equation [31]

$$\oint_{\partial\Omega} (\sigma.\mathbf{n})ds = \int_\Omega \rho \frac{du}{dt} d\Omega \tag{48}$$

with $\sigma = -p\delta + \tau$, p is the pressure, δ is the unity tensor, τ is the deviatoric stress tensor and $\mathbf{n}$ is the normal vector to the surface $\partial\Omega$.

Considering the geometry in Fig. 11, integration of the momentum equation gives the shear stress distribution,

$$\tau_{xy} = -p_x y. \tag{49}$$

For fully developed flow the momentum equation applied to the geometry of Fig. 11 states that

$$\underbrace{\int_a^b \tau_{xy} dx}_{upper\ wall} - \underbrace{\int_a^b -\tau_{xy} dx}_{bottom\ wall} + \underbrace{\int_{-y}^y (\tau_{xxa} - p_a) dx}_{left\ side} - \underbrace{\int_{-y}^y (\tau_{xxb} - p_b) dx}_{right\ side} = 0. \tag{50}$$

The stress profile is linear across the channel and based on Eq. (49) the yield surface distances are given by

$$\pm h_0 = \tau_0/p_x = \tau_0 h/\tau_w \tag{51-a}$$

$$p_x = \tau_w/h \tag{51-b}$$

$$\pm h_0 = \tau_0 h/\tau_w \tag{51-c}$$

where τ_w with $\tau_w > 0$ is the stress at the walls ($y = \pm h$) and τ_0 is the yield stress.

To obtain the solution for the Herschel–Bulkley and the Robertson–Stiff models, we followed the procedure of [32], except that here the slip velocity is included. The two rheological models can be written depending on the stress invariant [32]

$$\begin{cases} \dot{\gamma} = \left(\frac{\tau_0}{\mu_0}\right)^{1/n} \left(\frac{|\tau|}{\tau_0} - 1\right)^{1/n} \\ \dot{\gamma} = \left(\frac{\tau_0}{\mu_0}\right)^{1/n} \left(\left(\frac{|\tau|}{\tau_0}\right)^{1/n} - 1\right) \end{cases} \quad if\ |\tau| > \tau_0\ and\ (\dot{\gamma} = 0\ if\ |\tau| \leq \tau_0) \tag{52}$$

The flow rate dependence on the pressure gradient (direct problem) results from integration of the velocity profile over the domain (half of the domain because of symmetry) and leads to the following
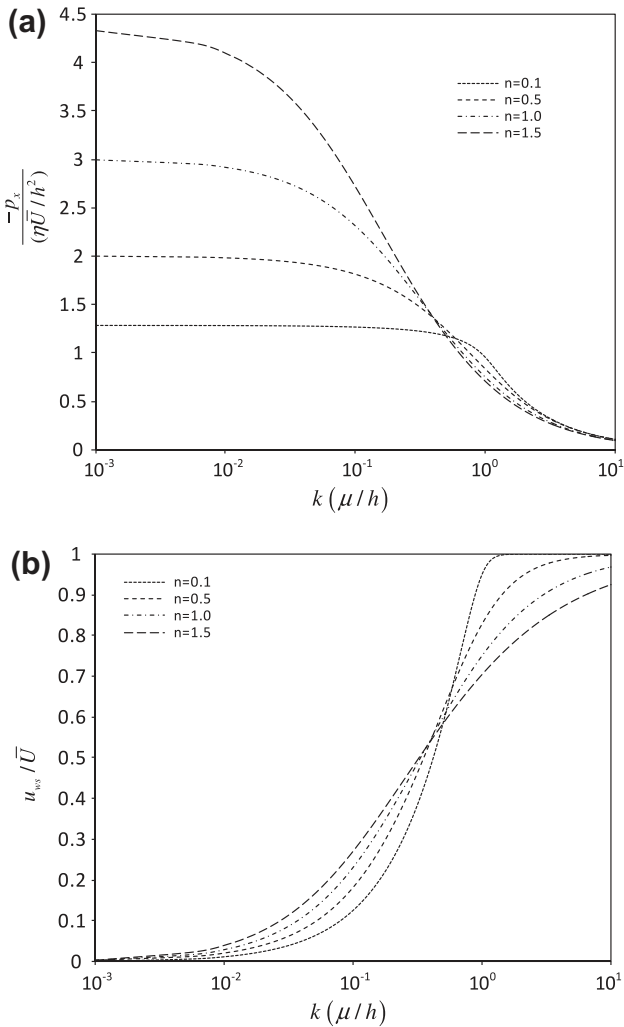
Fig. 9. Power law fluid with Navier slip boundary condition: (a) Normalized pressure drop versus slip coefficient (b) Normalized slip velocity versus slip coefficient.
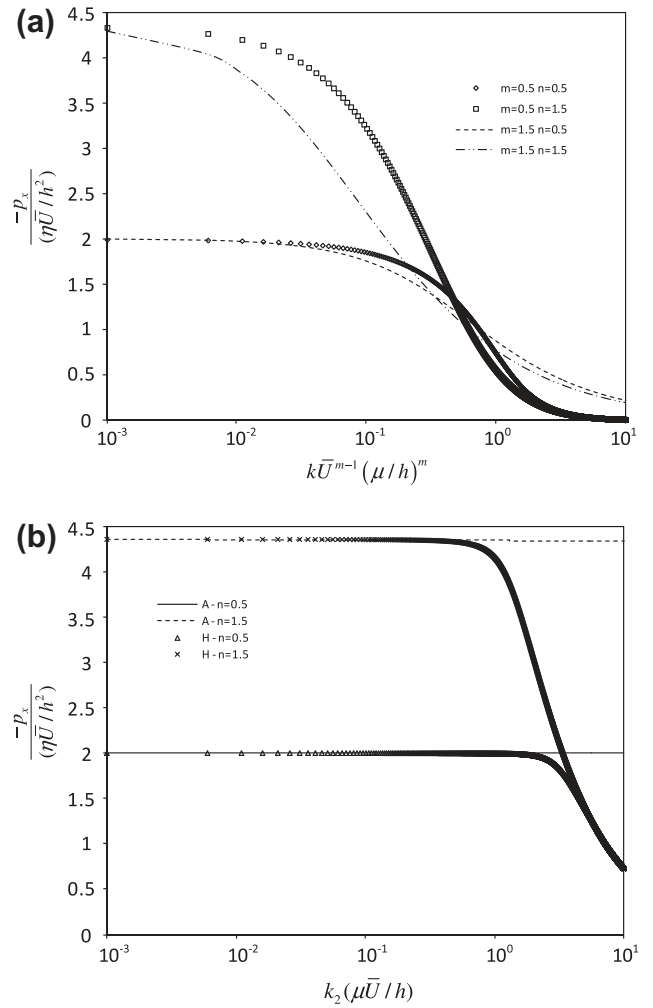

Fig. 10. (a)Pressure drop versus friction coefficient for different slip and power law exponents, (b) Pressure drop versus friction coefficient for the asymptotic and Hatzikiriakos slip models with $k'_1 = k_1/U = 1E - 3$, $k'_2 = k_2\eta U/h$.

velocity profiles (subscripts HB and RS stand for the Herschel–Bulkley and Robertson–Stiff models, respectively).

$$u(y)_{HB} = \begin{cases} u = \frac{n}{1+n}\left(\frac{p_x}{\mu_0}\right)^{1/n}[(h-h_0)^{(1+n)/n} - (y-h_0)^{(1+n)/n}] + u(h), & h_0 \leqslant |y| \leqslant h \\ u_{plug} = \frac{n}{1+n}\left(\frac{p_x}{\mu_0}\right)^{1/n}[(h-h_0)^{(1+n)/n}] + u(h), & 0 \leqslant |y| < h_0 \end{cases}$$

(53)

$u(y)_{RS}$
$$= \begin{cases} u = \left(\frac{\tau_0}{\mu_0}\right)^{1/n}(y-h) - \frac{n}{1+n}\left(\frac{p_x}{\mu_0}\right)^{1/n}[y^{(1+n)/n} - h^{(1+n)/n}] + u(h), & h_0 \leqslant |y| \leqslant h \\ u_{plug} = \left(\frac{\tau_0}{\mu_0}\right)^{1/n}(y-h) - \frac{n}{1+n}\left(\frac{p_x}{\mu_0}\right)^{1/n}[y^{(1+n)/n} - h^{(1+n)/n}] + u(h), & 0 \leqslant |y| < h_0 \end{cases}$$

(54)

To determine the inverse problem solution we impose a flow rate $Q = \overline{U}h$ and integrate over half of the channel width leading to the following solutions for the Herschel–Bulkley model

$$\frac{n}{1+n}\left(\frac{p_x}{\mu_0}\right)^{1/n}\left[h(h-h_0)^{(1+n)/n} - \frac{n[h-h_0]^{(1+2n)/n}}{1+2n}\right] + hu(h) - Q = 0$$

(55)

and the Robertson–Stiff model

Fig. 11. Geometry for the yield stress fluids. The plug zone goes from $-y_0$ to y_0. The channel width is $2h$.

$$\frac{n\left(\frac{\tau_0}{\mu_0}\right)^{1/n}(h_0)^{-1/n}}{1+2n}\left(h^{1/n+2} - (h_0)^{1/n+2}\right) - \frac{1}{2}\left(\frac{\tau_0}{\mu_0}\right)^{1/n}\left(h^2 - (h_0)^2\right)$$
$$+ hu(h) - Q = 0$$

(56)

respectively. In both cases $h_0 = \tau_0/p_x$ and the non-linear equations must be solved numerically.

Bingham fluids:

For the special case of Bingham fluids (Herschel–Bulkley model with $n = 1$) with Navier slip boundary condition, the full analytical solution is possible and is given by Eq. (57) for the direct problem

Table 6
Different values of $y_0 = \tau_0/\tau_w$ (dimensionless) for different slip coefficients $k_b = k\tau_0/\overline{U}_0$.

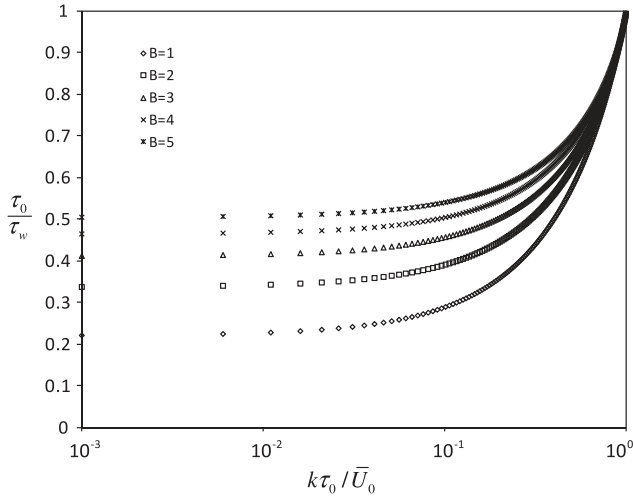| k_B	$B = 1$	$B = 2$	$B = 3$	$B = 4$	$B = 5$
l.OE−03	0.224140	0.340408	0.414660	0.467481	0.507620
l.OE−02	0.230245	0.345188	0.418678	0.470997	0.510775
l.OE−01	0.291645	0.393487	0.459390	0.506685	0.542850
l.OE+00	1.000000	1.000000	1.000000	1.000000	1.000000
l.OE+01	4.708312	3.798070	3.389721	3.146795	2.982333

Fig. 12. Variation of $y_0 = \tau_0/\tau_w$ with the (dimensionless) slip coefficient $k_B = k\tau_0/\overline{U}_0$.

$$u'(y') = \begin{cases} u_{fluid} = \frac{B}{2x}\left[(1-x)^2 - (|y'|-x)^2\right] + k_b, & x \le |y| \le 1 \\ U_{plug} = \frac{B}{2x}(1-x)^2 + k_B, & 0 \le |y| < x \end{cases}$$
(57)

and by Eq. (58) for the inverse problem

$$\underbrace{\frac{\tau_0^3(B/6)}{6\mu_0}}_{a} x^3 - \underbrace{(B/2 + 1)}_{b} x + \underbrace{B/3 + k_B}_{c} = 0$$
(58)

where B is the Bingham number $B = \tau_0 h/\mu_0\overline{U}_0$, $x = \tau_0/\tau_w$, $k_B = k\tau_0/\overline{U}_0$. The algebraic solution of this cubic equation is given as Eq. (59) with $p = b/a$ and $q = c/a$.

$$x = \sqrt[3]{-q/2 + \sqrt{(q/2)^2 + (p/3)^2}} + \sqrt[3]{-q/2 - \sqrt{(q/2)^2 + (p/3)^2}}.$$
(59)

Note that this solution is presented in the literature [31] in the absence of slip. Analytical solutions for Bingham fluids with Navier slip boundary conditions could be found for the special case of squeeze flow between parallel disks for the regularized bi-viscosity model with imposed pressure gradient [14]; a similar study is also given by [33].

4.4.1. Discussion (non-Newtonian fluids with yield stress)

For the yield stress fluids, the Bingham fluid was chosen. The studies were made varying the parameters B and k_B.

Fig. 12 shows the dramatic increase of stress ratio τ_0/τ_w with the slip coefficient, which means that the pressure gradient decreases and the plug size increases. The stress ratio τ_0/τ_w also decreases with the increase of the Bingham number. As the slip coefficient increases the plug grows in size towards the wall and it is not always possible to have a solution (un-yielded fluid). In

fact the yield stress cannot exceed the wall stress. Table 6 shows that for some values of k_B this condition is violated and this can bring problems to numerical simulation.

5. Conclusion

Analytical and semi-analytical solutions were presented for the direct and inverse flow problems of Couette–Poiseuille flows of Newtonian and non-Newtonian fluids. As for the non-Newtonian fluids, but for the latter only inelastic models were considered namely the power law, Sisko and two yield stress fluid models (Herschel–Bulkley and Robertson–Stiff). Four different slip models were considered, namely the Navier linear and non-linear slip laws, the asymptotic law and the Hatzikiriakos slip law. For some fluids, only particular solutions were presented, as for the Sisko fluid, whereas for cases, where the solution could not be found analytically, the existence of the solution was proven, and the interval, where the solution lies was given.

The proposed analytical solutions are valid for any values of the employed models' parameters, thus they cover all the slip velocity data given in the literature both for Newtonian and non-Newtonian fluids.

Acknowledgements

Appendix A. Couette flow of Newtonian fluids with non-linear Navier slip at the bottom wall and no-slip at the top wall

In the non-linear Navier slip law the boundary conditions are given by

$$u(-h) = k(\mu c_1)^m$$
(A.1)

$$u(h) = U$$
(A.2)

This implies that the constant $c_1 = \frac{U - k(\mu c_1)^m}{2h} \iff (c_1)^m + (2h/k\mu^m)c_1 - (U/k\mu^m) = 0$.

For $m = 0.5$ this non-linear equation can be solved with the help of a variable change $c_1^{0.5} = x \Rightarrow x^2 = c_1$, $x \ge 0$ leading to the equation

$$(2h/k\mu^m)x^2 + x - (U/k\mu^m) = 0,$$
(A.3)

which needs to be solved for the positive solution.

For $m = 2$ the solution is trivial and for $m = 3$ the Cardan–Tartaglia formula is used.

Remark. The solution c_1 is always positive. Let $f(c_1)$ be a function of the constant c_1 and given by $f(c_1) = (c_1)^m + (2h/k\mu^m)c_1 - (U/k\mu^m)$. The derivative of $f(c_1)$ is $f'(c_1) = m(c_1)^{m-1} + (2h/k\mu^m)$. It can also be seen that $f'(c_1) > 0, \forall c_1 \ge 0$, $f(0) < 0$ and that $f([U/k\mu^m]^{1/m}) > 0$. We can now conclude by Bolzano and Rolle theorems that there is a unique solution c_1 to equation $f(c_1) = 0$, in the range, $[0; [U/k\mu^m]^{1/m}]$.

Appendix B. Poiseuille flow of a Newtonian fluid with non-linear slip laws

For $m = 0.5, 1, 2$ and 3, a full analytical solution can be obtained and is given in Table 2.

The existence of a unique solution can be proved provided $m > 0$. The derivative of Eq. (33) is given by

$$-\frac{h^2}{3\mu} - mkh^m(-p_x)^{m-1} < 0, \; \forall p_x < 0 \tag{B.1}$$

Let

$$f(p_x) = -\frac{p_x}{3\mu}h^2 + kh^m(-p_x)^m - \overline{U}. \tag{B.2}$$

Then $f(0) = -\overline{U}$ and $f(-3\overline{U}\mu/h^2) = kh^m(3\overline{U}/h^2)^m > 0$, $f(-\overline{U}^{1/m}/kh^m) = \overline{U}^{1/m}h^2/(3\mu kh^m) > 0$. By Bolzano and Rolle theorems there is a unique solution in the range $]0; A[$ with $A = \min\{-3\overline{U}\mu/h^2; -\overline{U}^{1/m}/kh^m\}$.

Appendix C. Derivation of equations for different slip coefficients at top and bottom walls

Assume for the top wall the Navier slip boundary condition of Eq. (C1) and at the bottom wall the non-linear Navier slip law of Eq. (C.2)) with $m = 2, 3$.

$$u(h) = k_1(-p_x h - \mu c_1) \tag{C.2}$$

$$u(-h) = k_2(-p_x h + \mu c_1)^m \tag{C.3}$$

The system of equation that needs to be solved is (C.3)

$$-2hc_1 + u(h) - u(-h) = 0. \tag{C.3-a}$$

$$-\frac{p_x}{3\mu}h^2 - c_1 h + u(h) - U = 0. \tag{C.3-b}$$

where Eq. (C.3-b) is independent of the slip exponent and can be solved for the pressure gradient

$$p_x = \frac{c_1 h + k_1 \mu c_1 + U}{-k_1 h - \frac{h^2}{3\mu}} \tag{C.4}$$

By substitution of (C.4) into (C.3-a) a quadratic and a cubic equation are obtained for c_1 for $m = 2$ and 3, respectively.

The solution for $m = 2$ is given by (C.3) with constants (C.4) and (C.5)

$$c_1 = (16k_2\mu^2(1.5k_1\mu + h)^2)^{-1}(\sqrt{24}[(3k_1\mu + h)^2(1.5k_1^2\mu^4 k_2 U + 2.5k_2\mu^3 k_1 Uh + h^2\mu^2[k_2 U + (1/6)k_1^2] + (1/6)h^3 k_1\mu + (1/24)h^4)]^{0.5} -18k_2\mu^3 k_1 U + (-6k_1^2 - 12k_2 U)h\mu^2 - 5h^2 k_1\mu - h^3) \tag{C.5}$$

For $m = 3$ one has to solve the equation

$$c_1^3 + bc_1^2 + cc_1 + d = 0 \tag{C.6}$$

with coefficients

$$b = \frac{B}{A}, c = \frac{C}{A}, d = \frac{D}{A}$$
$$A = 288k_2\mu^4 h^2 + 432k_2\mu^5 hk_1^2 + 64k_2\mu^3 h^3 + 216k_2\mu^6 k_1^3$$
$$B = 432k_2\mu^4 hk_1 U + 144k_2\mu^3 h^2 U + 324k_2\mu^5 k_2 U$$
$$C = 16h^3 k_1\mu + 42h^2 k_1^2\mu^2 + 36hk_1^3\mu^3 + 108k_2\mu^3 hU^2 + 162k_2\mu^4 k_1 U^2 + 2h^4$$
$$D = -3k_1\mu Uh^2 - 18k_1^2\mu^2 Uh + 27k_2\mu^3 U^3 - 27k_1^3\mu^3 U$$

Making the substitution $c_1 = x - b/3$ the equation transforms to $x^3 + ex + f = 0$, and the so called Vieta substitution $x = y - e/3y$, leads to a quadratic equation for y^3.

$$(y^3)^2 + fy^3 - e^3/27 = 0 \tag{C.7}$$

This equation gives six solutions that reduce to three after back substitution.

Appendix D. Proof of existence of a unique solution for Poiseuille flows of power law fluids with slip

Let $f(p_x)$ be given by Eq. (D1) and $u(h)$ be given by Eqs. (20-a), (21-a) and (22-a)

$$f(p_x) = \left(\frac{-p_x}{a}\right)^{1/n}\left[\frac{h^{(1/n)+1}}{(1/n)+2}\right] + u(h) - \overline{U} \tag{D.1}$$

Let $f'(p_x)$ represent the derivative of function $f(p_x)$

$$f'(p_x) = \left[\frac{h^{(1/n)+1}}{((1/n)+2)an}\right]\left(\frac{-p_x}{a}\right)^{1/n-1} + \frac{du(h)}{dp_x} < 0, \; \forall p_x < 0 \tag{D.2}$$

Then $\frac{du(h)}{dp_x}$ is negative and is given by,

$$-mkh^m(-p_x)^{m-1} < 0 \tag{D.3}$$

$$-k_1 k_2 h \cosh(-k_2 p_x h) < 0 \tag{D.4}$$

$$\frac{-k_1 k_2 h}{1 - k_2 p_x h} < 0 \tag{D.5}$$

for the non-linear Navier, asymptotic and Hatzikiriakos slip models, respectively.

For all cases $f(0) = -\overline{U}$ and $f\left(-a\left[\frac{\overline{U}((1/n)+2)}{h^{(1/n)+1}}\right]^n\right) > 0$, $f(-\overline{U}^{1/m}/kh^m) = \overline{U}^{1/m}h^2/(3\mu kh^m) > 0$.

Regarding now the application of the slip condition, we have the following three models:

Non-linear Navier slip law:
$f(-\overline{U}^{1/m}/kh^m) = \overline{U}^{1/m}h^2/(3\mu kh^m) > 0$. By Bolzano and Rolle theorems there is a unique solution in the range $]0; A[$, $A = \min\left\{-a\left[\frac{\overline{U}((1/n)+2)}{h^{(1/n)+1}}\right]^n; -\overline{U}^{1/m}/kh^m\right\}$.

Hatzikiriakos slip law:
$f((-\text{arcsinh}(\overline{U}/k_1))/hk_2) > 0$. There is unique solution is in the range $]0; A[$ with $A = \min\{-a[\frac{\overline{U}((1/n)+2)}{h^{(1/n)+1}}]^n; -\text{arcsinh}(\overline{U}/k_1))/hk_2\}$.

Asymptotic slip law:
$f(-[\exp(\overline{U}/k_1) - 1]/hk_2) > 0$. There is a unique solution is in the range $]0; A[$ with $A = \min\left\{-a\left[\frac{\overline{U}((1/n)+2)}{h^{(1/n)+1}}\right]^n; -[\exp(\overline{U}k_1) - 1]/hk_2\right\}$.

Power-law Case ($n = 1/2$) **with Linear Slip** from Hatzikiriakos and Mitsoulis [28].

Their Eq. (11) is now simplified and given by,

$$\Delta p = \frac{B}{2A}\left[\frac{1}{R_L} - \frac{1}{R_0}\right]$$
$$- \left(\frac{R_0(B^2 R_0 + 4QA)\sqrt{\frac{B^2 R_0 + 4QA}{A^2 R_0^5}} - R_1(B^2 R_1 + 4QA)\sqrt{\frac{B^2 R_1 + 4QA}{A^2 R_1^5}}}{12QA}\right) \tag{D.6}$$

Appendix E. Derivation of analytical solution for Sisko model

The Sisko model is given by Eq. (7) and its substitution into the integrated form of the momentum equation (Eq. (5)) gives

$$\mu_\infty \frac{du}{dy} + a\left(\frac{du}{dy}\right)^n - p_x y = 0 \tag{E.1}$$

It is difficult to obtain the solution of this equation, because of its non-linear nature associated with the exponent, unless some particular values are explored such as $n = 0.5, 1$ and 2.

For $n = 0.5$ Eq. (E1) is quadratic on $\partial u/\partial y$. Let $x = (du/dy)^{0.5}$ leading to

$$\mu_\infty x^2 + ax - p_x y = 0 \tag{E.2}$$

The solutions of Eq. (E2) are given by Eq. (E3)

$$x = -\frac{a}{2\mu_\infty} \pm \frac{1}{2\mu_\infty}\sqrt{a^2 + [4\mu_\infty p_x]y}. \tag{E.3}$$

In order to pick the physically acceptable solution, it should be noticed that $du/dy > 0$ at $y = -h$. Notice that $[4\mu_\infty p_x]y \geqslant 0$ for $y \in [-h, 0]$ (favorable pressure gradient is negative) and $\sqrt{a^2 + [4\mu_\infty p_x]y} > a^2$ leading to

$$\frac{du}{dy} = \frac{a^2}{2\mu_\infty^2} - \frac{a\sqrt{a^2 + [4\mu_\infty p_x]y}}{2\mu_\infty^2} + \frac{p_x y}{\mu_\infty}. \tag{E.4}$$

which implies that

$$u(y) = \int \frac{a^2}{2\mu_\infty^2} - \frac{a\sqrt{a^2 + [4\mu_\infty p_x]y}}{2\mu_\infty^2} + \frac{p_x y}{\mu_\infty}\,dy \tag{E.5}$$

After integration

$$u(y) = \frac{a^2}{2\mu_\infty^2}y + \frac{p_x y^2}{2\mu_\infty} - \frac{a}{12\mu_\infty^3 p_x}[a^2 + 4\mu_\infty p_x y]^{3/2} + c \tag{E.6}$$

and applying the slip boundary condition $u(-h)$, the constant c is revealed and the final solution, depending on the pressure gradient, is given by

$$u(y) = \frac{a^2(y+h)}{2\mu_\infty^2} + \frac{p_x(y^2 - h^2)}{2\mu_\infty}$$
$$+ \frac{a([a^2 - 4\mu_\infty p_x h]^{3/2} - [a^2 + 4\mu_\infty p_x y]^{3/2})}{12\mu_\infty^3 p_x} + u(-h) \tag{E.7}$$

The solution to the inverse problem is given by solving the following equation with p_x as a variable

$$\frac{a^2 h}{4\mu_\infty^2} - \frac{p_x h^2}{3\mu_\infty} + \frac{a[a^2 - 4\mu_\infty p_x h]^{3/2}}{8\mu_\infty^3 p_x} + \frac{a([a^2 - 4\mu_\infty p_x]h^{5/2} - a^5)}{120h[\mu_\infty^2 p_x]^2}$$
$$+ u(-h) - \overline{U} = 0 \tag{E.8}$$

For $n = 1$ the solution is exactly the same as the one obtained for the Poiseuille flow and Newtonian fluid, but $\eta_0 + a$ should be used instead of μ.

For $n = 2$ the integrated momentum equation is again quadratic

$$a\left(\frac{du}{dy}\right)^2 + \mu_\infty \frac{du}{dy} - p_x y = 0 \tag{E.9}$$

and its solution is given by

$$\frac{du}{dy} = -\frac{\mu_\infty}{2a} \pm \frac{1}{2a}\sqrt{(\mu_\infty)^2 + [4ap_x]y}. \tag{E.10}$$

Proceeding as for the case $n = 0.5$ one has that

$$u(y) = \int -\frac{\mu_\infty}{2a} + \frac{1}{2a}\sqrt{(\mu_\infty)^2 + [4ap_x]y},\,dy + c$$
$$\iff u(y) = -\frac{\mu_\infty}{2a}y + \frac{1}{24a^2 p_x}[(\mu_\infty)^2 + 4ap_x y]^{3/2} + c \tag{E.11}$$

Applying the boundary condition $u(-h)$, we find the final solution depending on the pressure gradient

$$u(y) = \frac{\mu_\infty}{2a}(-y - h) + \frac{[(\mu_\infty)^2 + 4ap_x y]^{3/2} - [(\mu_\infty)^2 - 4ap_x h]^{3/2}}{12a^2 p_x} + u(-h) \tag{E.12}$$

The solution to the inverse problem is given by the following equation with p_x as a variable

$$-\frac{\mu_\infty}{4a}h - \frac{[(\mu_\infty)^2 - 4ap_x h]^{3/2}}{12a^2 p_x} + \frac{[(\mu_\infty)^5 - ((\mu_\infty)^2 - 4ap_x y)^{5/2}]}{120ha^3 p_x}$$
$$+ u(-h) - \overline{U} = 0. \tag{E.13}$$

References

[1] M.M. Denn, Extrusion instabilities and wall slip, Ann. Rev. Fluid Mech. 33 (2001) 265–287.
[2] R. Berker, Integration des Equations du Mouvement d'un Fluide Visqueux, Incompressible, Handbuch der Physik, vol. VIII 2, Springer-Verlag, Berlin, 1963.
[3] R.B. Bird, C.F. Curtiss, R.C. Armstrong, O. Hassager, Dynamics of Polymeric Liquids, vol. 2, John Wiley and Sons, New York, 1987.
[4] E. Lauga, M.P. Brenner, H.A. Stone, in: C. Tropea, A. Yarin, J.F. Foss (Eds.), Handbook of Experimental Fluid Dynamics, Springer, 2007, pp. 1219–1240 (Chapter 19).
[5] S.G. Hatzikiriakos, Wall slip of molten polymers, Prog. Polym. Sci. (2011), http://dx.doi.org/10.1016/j.progpolymsci.2011.09.04.
[6] H. Meijer, C. Verbraak, Modeling of extrusion with slip boundary conditions, Polym. Eng. Sci. 28 (1988) 758–772.
[7] H. Potente, H. Ridder, R.V. Cunha, Global concept for describing and investigation of wall slip effects in the extrusion process, Macromol. Mater. Eng. 11 (2002) 836–842.
[8] H. Potente, K. Timmermann, M. Kurte-Jardin, Description of the pressure/ throughput behavior of a single-screw plasticating unit in consideration of wall slippage effects for non-newtonian material and 1-D flow, Int. Polym. Process. 21 (2006) 272–281.
[9] M. Chatzimina, G. Georgiou, K. Housiadas, S.G. Hatzikiriakos, Stability of the annular Poiseuille flow of a Newtonian liquid with slip along the walls, J. Non-Newtonian Fluid Mech. 159 (2009) 1–9.
[10] R. Ellahi, T. Hayat, F.M. Mahomed, A. Zeeshan, Exact solutions for flows of an Oldroyd 8-constant fluid with nonlinear slip conditions, Commun. Nonlin. Sci. Numer. Simulat. 15 (2009) 322–330.
[11] Y.H. Wu, B. Wiwatanapataphee, M.B. Hu, Pressure-driven transient flows of Newtonian fluids through microtubes with slip boundary, Phys. A: Stat. Mech. Appl. 387 (2008) 5979–5990.
[12] M.T. Matthews, J.M. Hill, Newtonian flow with nonlinear Navier boundary condition, Acta Mech. 191 (2007) 195–217.
[13] P.A. Thompson, S.M. Troian, A general boundary condition for liquid flow at solid surfaces, Nature 389 (1997) 360–362.
[14] S.P. Yang, K.Q. Zhu, Analytical solutions for squeeze flow of Bingham fluid with Navier slip condition, J. Non-Newtonian Fluid Mech. 138 (2006) 173–180.
[15] H. Fujita, A coherent analysis of Stokes flows under boundary conditions of friction type, J. Comp. Appl. Math. 149 (2002) 57–69.
[16] C. Le Roux, A. Tani, Steady solutions of the Navier–Stokes equations with threshold slip boundary conditions, Math. Meth. Appl. Sci. 30 (2007) 595–624.
[17] A. de Waele, Viscometry and plastometry, J. Oil Colour Chem. Assoc. 6 (1923) 33–88.
[18] A.W. Sisko, Flow of lubricating greases, Ind. Eng. Chem. 50 (1958) 1789–1792.
[19] W.H. Herschel, R. Bulkley, Konsistenzmessungen von Gummi-Benzollösungen, Kolloid Zeitschrift 39 (1926) 291–300.
[20] R.E. Robertson, H.A. Stiff, An improved mathematical model for relating shear stress to shear rate in drilling fluids and cement slurries, Soc. Pet. Eng. J. 16 (1976) 31–36.
[21] H. Lamb, Hydrodynamics, sixth ed., Cambridge University Press, Cambridge, UK, 1932.
[22] G.K. Batchelor, An Introduction to Fluid Dynamics, Cambridge University Press, Cambridge, UK, 1967.
[23] S. Goldstein, Modern Developments in Fluid Dynamics: An Account of Theory and Experiment Relating to Boundary Layers, vol. 1, Turbulent Motion and Wakes, New York, Dover, 1965.
[24] E. Mitsoulis, I.B. Kazatchkov, S.G. Hatzikiriakos, The effect of slip in the flow of a branched PP melt: experiments and simulations, Rheol. Acta 44 (2005) 418–426.
[25] C.L.M.H. Navier, Memoire sur les lois du mouvement des fluids, Mem. Acad. Roy. Sci. Inst. Fr. 6 (1827) 389–440.
[26] W.R. Schowalter, The behavior of complex fluids at solid boundaries, J. Non-Newtonian Fluid Mech. 29 (1988) 25–36.
[27] S.G. Hatzikiriakos, A slip model for linear polymers based on adhesive failure, Intern. Polym. Process. 8 (1993) 135–142.
[28] ANSYS Polyflow manual (implementation of boundary conditions), 2011, ANSYS.
[29] S.G. Hatzikiriakos, E. Mitsoulis, Slip effects in tapered dies, Polymer Engineering and Science 49 (2009) 1960–1969.
[30] R.B. Bird, W.E. Stewart, E.N. Lightfoot, Transport Phenomena, second ed., John Wiley and Sons, New York, 2002.
[31] I.A. Frigaard, S.D. Howison, I.J. Sobey, On the stability of Poiseuille flow of a Bingham fluid, J. Fluid Mech. 263 (1994) 133–150.
[32] E.J. Fordham, S.H. Bittleston, M.A. Tehrani, Viscoplastic flow in centered annuli, pipes, and slots, Ind. Eng. Chem. 30 (1991) 517–524.
[33] P. Estelle, C. Lanos, Squeeze flow of Bingham fluids under slip with friction boundary conditions, Rheolog. Acta 46 (2007) 397–404.